Std Solar Model

A model of the sun at present is called a "standard solar model". How do we make one?

- We know $R_\odot$, $L_\odot$, $Z = 1 - X - Y$ from direct observation
- We estimate $t_\odot$ from various sources (eg radioactivity in Earth rocks, meteorites etc)

Unknowns are:

- X (or Y)
- $\alpha = l_{mix} / H_p$

  = mixing-length parameter in the convection theory

  l_{mix} = mixing-length = mean-free-path of an eddy

  H_p = pressure-scale height = distance over which P changes by a factor $1/e$ (if H_p is constant)

  $$= -\frac{dr}{d\ln P} = -\frac{P\,dr}{dP}$$

As you know from the Assignment, you vary X and α and run the code until $t_\odot$. Then compare L with $L_\odot$ and R with $R_\odot$. Iterate on X and α until it gives the correct L & R.

<u>Checks</u>: the study of helioseismology now gives us much more information about the Sun's interior than was ever available before. We now know the run of c^2 (sound-speed $= c$) through the Sun to very high accuracy, and it matches the Std model very well.

Similarly, helioseismology identifies the position of the bottom of the convective envelope and that agrees well too! It also tells us the Y value there – and this can only be matched if we allow for gravity to slowly diffuse He through the atmosphere slightly.

Neutrinos

Neutrinos from nuclear reactions have been detected for years - the high energy ν were all that could be measured for a long time. These came from the Be^7, B^8 branch of PP<u>III</u>, and were measured at a rate ~1/3 predicted. Recently we tested the PPI reaction

$$H^1 + H^1 \rightarrow D^2 + \beta^+ + \nu$$

which is very low energy ν, and this required lots of Gallium to build the detector. If <u>THIS</u> first reaction in PP is wrong, then how can we trust the rest (which are further down the chain and have compounded uncertainties). The rate measured was ~1/2 predicted.

Stellar evolution theorists have made all sorts of strange models to try to accommodate these measurements. None have worked....

One possibility is that ν_e change into ν_μ and ν_τ somehow. It is ν_e that are made in the Sun, and ν_e that are measured. If some have "mixed" into ν_μ & ν_τ then we would not detect them.

Recently (2001!) it was possible to measure one of these other kinds, using a new detector SNO = Sudbury Neutrino Observatory in Canada. The total matched the theory!

The "Solar Neutrino Problem", which existed for ~~40~~ 30 years, is solved. The models are correct, it's the neutrino that behaves strangely!

Lattanzio & Boothroyd 1997

the evolution up to the beginning of thermal pulses on the AGB (the so-called "TP-AGB"), with a brief discussion of further evolution (for which a more detailed discussion is given in section IV).

A Basic Evolution at 1 Solar Mass

We make the usual assumption that a star reaches the zero-age main sequence with a homogeneous chemical composition. Figure 1 shows a schematic HR diagram for a $\sim 1\,M_\odot$ star. Core H-burning occurs radiatively, and the central temperature and density grow in response to the increasing molecular weight (points 1–3) until central H exhaustion (point 4). The H profiles are shown in inset (a) in Figure 1. The star now leaves the main sequence and crosses the Hertzsprung Gap (points 5–7), while the central ^{4}He-core becomes electron degenerate and the nuclear burning is established in a shell surrounding this core. Inset (b) shows the advance of the H-shell during this evolution. Simultaneously, the star is expanding and the outer layers become convective. As the star reaches the Hayashi limit ($\sim$ point 7), convection extends quite deeply inward (in mass) from the surface, and the star ascends the (first) red giant branch (RGB). The convective envelope penetrates into the region where partial H-burning has occurred earlier in the evolution, as shown in inset (c) of Figure 1. This material is still mostly H, but with added ^{4}He together with the products of CN cycling, primarily ^{14}N and ^{13}C. These are now mixed to the surface (point 8) and this phase is known as the "first dredge-up". The most important surface abundance changes are an increase in the ^{4}He mass fraction by about 0.03 (for masses less than about $4M_\odot$), while ^{14}N increases at the expense of ^{12}C by around 30%, and the number ratio ^{12}C/^{13}C drops from its initial value of ~ 90 to lie between 18 and 26 [13]. Further details are given in section III below.

As the star ascends the giant branch the ^{4}He-core continues to contract and heat. Neutrino energy losses from the centre cause the temperature maximum to move outward, as shown in inset (d) of Figure 1. Eventually triple alpha reactions are ignited at this point of maximum temperature, but with a degenerate equation of state. The temperature and density are decoupled: the resulting ignition is violent, and is referred to as the "core helium flash" (point 9: see for example [16]). Following this, the star quickly moves to the Horizontal Branch where it burns ^{4}He gently in a convective core, and H in a shell (which provides most of the luminosity). This corresponds to points 10–13 in Figure 1. Helium burning increases the mass fraction of ^{12}C and ^{16}O (the latter through ^{12}C$(\alpha,\gamma)^{16}$O) and the outer regions of the convective core become stable to the Schwarzschild convection criterion but unstable to that of Ledoux: a situation referred to as "semiconvection" (space prohibits a discussion of this phenomenon, but an excellent physical description is contained in [10,11]). The semiconvection causes the composition profile to adjust

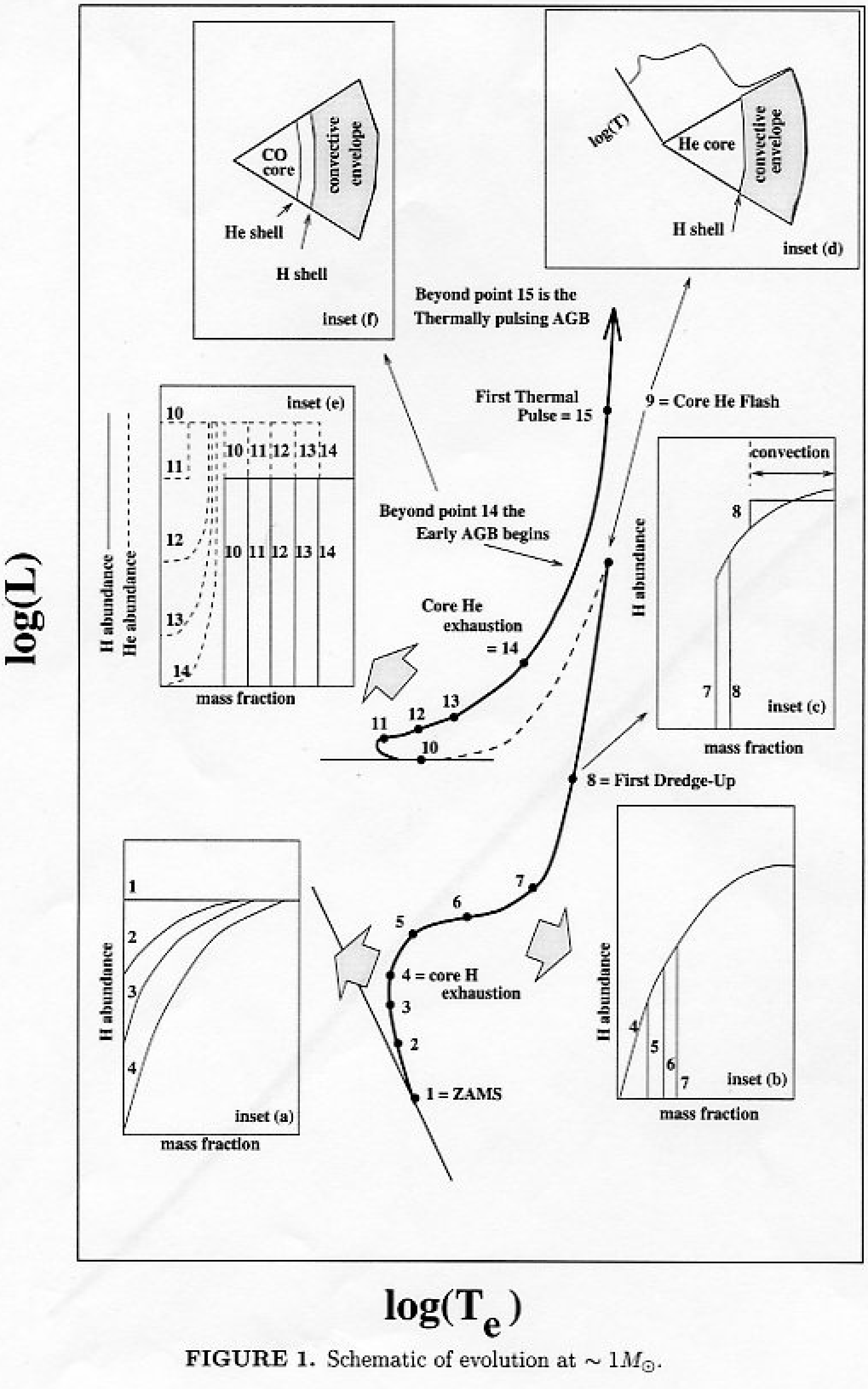

FIGURE 1. Schematic of evolution at $\sim 1 M_{\odot}$.

itself to produce convective neutrality, with the resulting profiles as shown in inset (e) of Figure 1.

Following ^{4}He exhaustion (point 14), the star ascends the giant branch for the second time, and this is known as the Asymptotic Giant Branch, or AGB, phase. The final proportions of ^{12}C and ^{16}O in the ^{4}He-exhausted core depend on the uncertain rate for the $^{12}\mathrm{C}(\alpha,\gamma)^{16}\mathrm{O}$ reaction. The core now becomes electron degenerate, and the star's energy output is provided by the ^{4}He-burning shell (which lies immediately above the C-O core) and the H-burning shell. Above both is the deep convective envelope. This structure is shown in inset (f) in Figure 1. We will later see that the ^{4}He-shell is thermally unstable, as witnessed by the recurring "thermal pulses". Thus the AGB is divided into two regions: the early-AGB (E-AGB), prior to (and at lower luminosities than) the first thermal pulse, and the thermally-pulsing AGB (TP-AGB) beyond this. We will return to this in section IV.

B Basic Evolution at 5 Solar Masses

A more massive star, say of $5M_\odot$, begins its life very similarly to the lower mass star discussed above. The main initial difference is that the higher temperature in the core causes CNO cycling to be the main source of H-burning, and the high temperature dependence of these reactions causes a convective core to develop. As H is burned into ^{4}He the opacity (mainly owing to electron scattering, and hence proportional to the H content) decreases and the extent of the convective core decreases with time. This corresponds to points 1–4 in Figure 2. Following core H exhaustion there is a phase of shell burning as the star crosses the Hertzsprung Gap (points 5–7 and inset (b)), and then ascends the (first) giant branch. Again the inward penetration of the convective envelope (point 8) reaches regions where there has been partial H-burning earlier in the evolution, and thus these products (primarily ^{13}C and ^{14}N, produced at the cost of ^{12}C) are mixed to the surface in the first dredge-up, just as seen at lower masses, and sketched in inset (c) of Figure 2.

For these more massive stars the ignition of ^{4}He occurs in the centre and under non-degenerate conditions, and the star settles down to a period of quiescent ^{4}He-burning in a convective core, together with H-burning in a shell (see inset (d) in Figure 2). The competition between these two energy sources determines the occurrence and extent of the subsequent blueward excursion in the HR diagram [48], when the star crosses the instability strip and is observed as a Cepheid variable (points 10–14). Following core ^{4}He exhaustion, the structural readjustment to shell ^{4}He burning results in a strong expansion, and the H-shell is extinguished as the star begins its ascent of the AGB. With this entropy barrier removed, the inner edge of the convective envelope is free to penetrate the inactive H-shell. Thus the products of complete H-burning are mixed to the surface in what is called the "second dredge-up" (point 15).

Relevant sections marked | |

THE ASTROPHYSICAL JOURNAL, 360: 727–736, 1990 September 10

OUR SUN. I. THE STANDARD MODEL: SUCCESSES AND FAILURES[1]

I.-JULIANA SACKMANN, ARNOLD I. BOOTHROYD,[2] AND WILLIAM A. FOWLER
W. K. Kellogg Radiation Laboratory, California Institute of Technology
Received 1989 December 15; accepted 1990 March 9

ABSTRACT

We have computed a number of standard solar models. Our best Standard Sun has $Y = 0.278$, $Z = 0.0194$, and $\alpha = 2.1$, using $L_\odot \equiv 3.86 \times 10^{33}$ ergs s^{-1}, $R_\odot \equiv 6.96 \times 10^{10}$ cm, $t_\odot = 4.54$ Gyr, and the value of $Z/X = 0.02766$ published by Grevesse in 1984; we used LAOL opacities, including molecular opacities, nuclear rates published by Caughlin and Fowler in 1988, and neutrino capture cross sections published by Bahcall and Ulrich in 1988. We predicted a ^{37}Cl neutrino capture rate of 7.7 SNUs, which would be observed if all solar neutrinos reach Earth (i.e., in the absence of such effects as the MSW neutrino oscillation effect which could reduce the flux of electron neutrinos). This is in agreement with results of other authors, but a factor of 4 larger than the average observed rate. We predict neutrino capture rates for other targets: 26 SNUs for ^{81}Br, 17 SNUs for ^{98}Mo, 125 SNUs for ^{71}Ga, 615 SNUs for ^{115}In, and 47 SNUs for ^{7}Li.

We have investigated the sensitivity of the standard solar model to uncertainties in the solar luminosity, solar age, and observed Z/X ratio as well as to changes in molecular opacities, pressure ionization effects in the envelope, and nonequilibrium ^{3}He energy contributions. Of these, only the uncertainty in Z/X has a significant effect on the solar Y value and the ^{37}Cl neutrino capture rate: use of the older value published by Ross and Aller in 1976 of $Z/X = 0.02282$ decreases Y by 0.014 and decreases the ^{37}Cl rate by 1.5 SNUs. While the 1989 work of Guenther, Jaffe, and Demarque has shown that Y can be significantly affected by the choice of stellar interior opacities, we find that even large changes in the *low-temperature molecular opacities* have *no* effect on Y, nor even on conditions at the *base* of the convective envelope. The large molecular opacities *do* cause a large increase in the mixing-length parameter α but do *not* cause the convective envelope to reach deeper. The temperature remains too low for lithium burning, and there is no surface lithium depletion, let alone the observed depletion of a factor of 100: the lithium problem of the standard solar model remains.

Subject headings: neutrinos — nucleosynthesis — Sun: interior

I. INTRODUCTION

The initial impetus for creating standard solar models came from our interest in creating nonstandard solar models. Guzik, Willson, and Brunish (1987) have produced very interesting nonstandard solar models: they considered the possibility of large amounts of mass loss during the early main-sequence stage. We wished to look at this possibility in more detail (see Boothroyd, Sackmann, and Fowler 1990, hereafter Paper II). A standard model was clearly required for comparison purposes. It is also of considerable interest in its own right. Therefore we made an effort to use the current (observed) solar composition values, as well as up-to-date input physics, nuclear reaction rates, and opacities.

The ratio Z/X of solar metallicity to solar hydrogen abundance is fairly well determined by observations. However, the solar helium abundance is not constrained very tightly. Another important quantity, which is not directly observable at all, is the parameter $\alpha \equiv l/H_p$, the ratio of the convective mixing length to the pressure scale height. This parameter determines the depth of the outer convective envelope and therefore strongly affects the radius of a stellar model. Fortunately, two key boundary conditions allow us to determine these quantities: the luminosity $L_\odot$ and radius $R_\odot$ of the Sun at the present age, which are relatively well determined by observations.

It has only recently been demonstrated conclusively (Guenther, Jaffe, and Demarque 1989) that the value obtained for the presolar helium abundance changes significantly (from $Y \approx 0.24$ to $Y \approx 0.28$) if one uses interior opacities from the Los Alamos Opacity Library (LAOL) rather than the older opacities of Cox and Stewart (1970). (This had been suspected earlier, from a comparison of solar models of different authors: see, e.g., Lebreton and Maeder 1986.) The molecular opacities at temperatures below about 10^4 K are still very uncertain; a number of recent authors have included molecular opacities, from a number of different sources (see discussion in § III). We wanted to investigate whether this uncertainty in the molecular opacity would also have a large effect on the solar models. There is some uncertainty in the solar composition, age, and luminosity, so we tested the effect of varying these also. We also tested the effect of adding pressure ionization effects ("depression of the continuum") to our model, and the effect of nonequilibrium ^{3}He burning on the nuclear energy production.

We constructed evolutionary tracks from the zero-age main sequence (ZAMS) up to the solar age. Each track requires an input value for the initial helium abundance Y and metallicity Z, as well as for the value of the mixing-length parameter α. Holding either Z or Z/X fixed, we varied Y and α until our tracks had the solar luminosity and effective temperature (and thus radius) at the solar age. This determined a unique value for Y, Z, and α for our Standard Sun. We could not resist exploring the Sun's future fate: for our best Standard Sun, we carried the evolution up through the red giant stage and core helium burning stage to the asymptotic giant branch stage.

[1] This work was supported in part by a grant from the National Science Foundation PHY-8817296.

[2] Now at the Canadian Institute for Theoretical Astrophysics, University of Toronto.

Details of this, and the future of the nonstandard solar models of Paper II, will be presented in Sackmann, Boothroyd, and Kraemer (1990, hereafter Paper III).

In § II we describe in more detail our methods, the input physics, and the measured and observed quantities. In § III we present our results for the Sun at its present age and compare our results with those of other authors. In § IV we summarize our conclusions and point out key uncertainties in the input physics, in the computing techniques, and in the observations.

II. METHOD

a) Nuclear Physics

Our stellar evolutionary program is described in some detail in Boothroyd and Sackmann (1988*a*). It already included nonequilibrium CNO burning, following ^{12}C, ^{14}N, ^{16}O and ^{18}O; for the solar work, we added the isotopes ^{13}C and ^{17}O. In addition, we added nonequilibrium burning of ^{3}He and ^{7}Li in the proton-proton chain, although for these we did not in general include the nonequilibrium effects on the energy generation rate. (Nonequilibrium ^{3}He energy generation *was* included in one of our solar models, but we were not completely satisfied that our algorithm for including this energy was stable enough numerically to give accurate results.) The nuclear burning rates were updated to values provided by Fowler (1987), which have since been published by Caughlan and Fowler (1988). Screening corrections are included, according to the prescription of Salpeter (1954).

b) Opacities

The opacities, as in our previous work (Boothroyd and Sackmann 1988*a*), were Rosseland mean opacities κ obtained from the Los Alamos Opacity Library (LAOL). We interpolated among these tables in metallicity Z and hydrogen abundance X in order to obtain the opacity corresponding to the composition at each point in our models: the opacity κ was interpolated linearly in Z and X. Keady (1985) supplied us with Los Alamos tables for hydrogen-rich ($X = 0.7$) and hydrogen-poor ($X = 0$) mixtures, for metallicities $Z = 0.02$, $Z = 0.001$, and $Z = 0.0001$. These tables include both *molecular* and atomic cross sections, as well as broadening due to turbulence (thermal and collisional broadening are also included, but are less important than tubulence broadening). The opacities due to a number of molecules are included, namely H^-, H_2, H_2^+, H_2^-, H_2O, N_2, CO, and CN. The following molecules were also included in the equation of state, but their opacities were not available yet: OH, C_2, O_2, NO, CO_2, NO_2, and CH. High-temperature ($T > 10^4$ K) Los Alamos opacities for $Z = 0.03$ and $X = 0.7$, $X = 0.3$, and $X = 0$ were obtained from Huebner (1976); low-temperature extensions to these tables were obtained by extrapolation in Z (see Sackmann and Boothroyd 1985) of Los Alamos opacity tables (with *molecular* effects included) that were published by Meyer-Hofmeister (1982). Note that the opacity tables of Huebner (1976) use the same heavy element *abundance* ratios as Cox and Stewart (1970) and thus are not compeltely consistent with the tables of Keady (1985), who used the heavy element abundance ratios of Ross and Aller (1976) (see Table 1). This inconsistency had no effect on the present work, since none of our models had a metallicity in excess of $Z = 0.02$, and therefore all models of the present work used the Keady (1985) opacities.

c) Solar Abundances

The ratio Z/X at the Sun's surface can be inferred from observations of the photospheric spectrum. Ross and Aller (1976) provided a table of the abundances of heavier elements relative to hydrogen, n_i/n_H; these can be used to obtain a value of $Z/X = 0.02282$. Typical quoted uncertainties in the major components of Z were of order 15%–30%, implying an uncertainty of roughly 20% in Z/X. More recently, the abundances reported by Grevesse (1984) yield a value of $Z/X = 0.027665$, while those of Aller (1986) yield $Z/X = 0.02739$. The quoted errors here are somewhat smaller; Grevesse (1984) quotes standard deviations of a few percent for the best-determined elements but gives no error estimate at all for those that may be less accurate. It seems reasonable to follow the lead of Bahcall and Ulrich (1988) and consider the difference (of about 19%) between the Ross and Aller (1976) value and the values of Grevesse (1984) and of Aller (1986) to be a 3 σ error. One thus infers a 1 σ error of about 6% in these more recent values of Z/X.

The relative contributions of the individual metals to the total metallicity (Z_i/Z) vary much less than the ratio Z/X from Ross and Aller (1976) to Grevesse (1984). The largest change is for Ne, up by more than a factor of 2 (which, however, is only 4% of Z); the others all change by less than 2% of Z (see Table 1). One should note that the Keady (1985) opacities used Z_i/Z values from Ross and Aller (1976), with the exception of the value for Fe, which lay about halfway between the Ross and Aller (1976) value and the Grevesse (1984) value. We used the Grevesse values of C/Z, N/Z, and O/Z for the initial composition of our models.

The initial CNO isotopic ratios were selected according to the observed solar system number ratios: $^{12}C/^{13}C = 90$ and $^{16}O/^{17}O = 2660$ (Dominy and Wallerstein 1987), and $^{16}O/^{18}O = 500$ (Dominy, Wallerstein, and Suntzeff 1986). The initial ^{7}Li abundance by mass was taken to be $X_{Li} = 4 \times 10^{-9}$, as implied by the number ratio $^{7}Li/H = 8 \times 10^{-10}$ obtained from observations of Population I stars (Boesgaard and Steigman 1985); this is also consistent with computations of big bang nucleosynthesis (see, e.g., Malaney and Fowler 1988). For initial ^{3}He, we used the solar system number ratio of $(^{2}H + {}^{3}He)/{}^{4}He = 4.0 \times 10^{-4}$ (Boesgaard and Steigman 1985); since our code does not follow deuterium explicitly, and since deuterium burns very rapidly to ^{3}He in the solar interior,

TABLE 1

COMPONENTS (by Mass) Z_i/Z OF THE SOLAR METALLICITY[a]

Element	$(Z_i/Z)_H$	$(Z_i/Z)_K$	$(Z_i/Z)_{RA}$	$(Z_i/Z)_G$	$(Z_i/Z)_G - (Z_i/Z)_{RA}$
C	0.1408	0.2179	0.2177	0.2110	−0.0067
N	0.0463	0.0531	0.0530	0.0491	−0.0041
O	0.4198	0.4816	0.4813	0.4664	−0.0149
Ne	0.2984	0.0326	0.0326	0.0724	+0.0398
Na	0.0014	0.0019	0.0019	0.0018	−0.0001
Mg	0.0180	0.0421	0.0421	0.0331	−0.0089
Al	0.0013	0.0039	0.0039	0.0029	−0.0010
Si	0.0264	0.0546	0.0546	0.0357	−0.0188
S	...	0.0230	0.0221	0.0187	−0.0034
Ar	0.0392	0.0017	0.0017	0.0054	+0.0037
Ca	...	0.0041	0.0039	0.0033	−0.0006
Fe	0.0085	0.0835	0.0768	0.0937	+0.0169

[a] Note that H refers to the Huebner 1976 mix, K to the Keady 1985 mix, RA to the Ross and Aller 1976 abundance observations, and G to the Grevesse 1984 abundance observations; the last column shows the difference between the abundances of Ross and Aller 1976 and those of Grevesse 1984.

we defined the initial number ratio of $^3He/^4He$ to be 4.0×10^{-4}.

d) Equation of State; Degeneracy and Pressure Ionization

The equation of state in the interior ($\log T > 6.3$ for our solar models) included a perfect gas with electron degeneracy effects and radiation pressure, and carbon and oxygen ionization effects (with full ionization of hydrogen and helium). The equation of state in the envelope included a perfect gas with radiation pressure and the partial ionization of hydrogen, helium, and carbon and the formation of H_2 molecules. Electron degeneracy and pressure ionization have only a very small effect in the Sun, but their effects are not completely negligible, so they were added to the envelope equation of state for one of the solar models of this work. The static envelope was based on the prescription of Paczyński (1969), which was modified as described in Sackmann and Boothroyd (1985) and Boothroyd and Sackmann (1988*a*). We included the effects of degeneracy in the static envelope according to a relatively simple prescription of Henyey, LeLevier, and Levee (1959), as corrected by Rappaport, Joss, and Webbink (1982). One may write the degeneracy-corrected electron pressure as

$$P_e = n_e k_B T\left(1 + \frac{F_{1/2}}{\sqrt{8\pi}(1 + bF_{1/2})^{1/3}}\right),$$

where

$$b = \frac{125}{144}(2\pi)^{-3/2}$$

and

$$F_{1/2} = \frac{\rho h^3}{4\pi m_H \mu_e (2m_e k_B T)^{3/2}} = \frac{n_e h^3}{4\pi (2m_e k_B T)^{3/2}} . \qquad (1)$$

This formula is good for *all* degeneracy levels; its maximum inaccuracy is a few percent, at intermediate degeneracy levels. In addition, the factor e^η (due to degeneracy) in the Saha ionization equation may be approximated by

$$e^\eta \approx y(1 + 0.3536y + 0.0576y^2), \quad \text{where } y = \frac{2}{\sqrt{\pi}} F_{1/2} . \qquad (2)$$

This is accurate to about 5% for $F_{1/2} \lesssim 2$. Pressure ionization was included via the prescription of Copeland, Jensen, and Jørgensen (1970) for "depression of the continuum" (see also Stewart and Pyatt 1966). In the Saha equation, the ionization energy of the rth ionization stage of an element was reduced by an amount Δ_r, given by

$$\Delta_r = k_B T\{[3(z^* + 1)K_r + 1]^{2/3} - 1\}\frac{f}{2(z^* + 1)},$$

where

$$K_r = \frac{z_r e^2}{r_D k_B T}, \quad z_r = r + 1, \quad z^* = \frac{\langle z^2 \rangle}{\langle z \rangle},$$

and

$$\frac{1}{r_D} = \left[\frac{4\pi e^2}{k_B T}\sum_i (z_i^2 + z_i)n_i\right]^{1/2} . \qquad (3)$$

Note that f is a factor of order unity, whose value varies between 0.95 and 1.2; we took it to be exactly unity. It should be noted that this method of "depression of the continuum" is not a fully self-consistent method for including pressure ionization. For this reason, we also ran an evolutionary track without pressure ionization, for comparison purposes (see § III). Recently, Hummer and Mihalas (1989), Däppen *et al.* (1989), and Mihalas, Däppen, and Hummer (1989) claim to have obtained a complete and self-consistent equation of state, which should clear up the uncertainties in the formulation of pressure ionization, but this should have little effect on solar models, since pressure ionization is a small effect in the Sun.

e) Solar Neutrinos

We created a separate routine to compute the neutrino flux at Earth's orbit from the neutrinos produced by the *p-p* chain and the CNO cycle (assuming the Sun to be completely transparent to neutrinos). Absorption cross sections from Table VII of Bahcall and Ulrich (1988) were used to compute the capture rate that would result for targets of ^7Li, ^{37}Cl, ^{71}Ga, ^{81}Br, ^{98}Mo, and ^{115}In.

The capture cross sections for neutrinos from the reaction $^{18}F(e^+, \nu)^{18}O$ were not given in Bahcall and Ulrich (1988). We estimated these cross sections by interpolating in the capture cross sections for neutrinos produced by the *p-p*, ^{13}N, ^{17}O, and ^{17}F reactions as a function of the Q-value of these reactions. Since the flux of ^{18}F neutrinos is negligible, uncertainties in the capture cross sections for ^{18}F neutrinos have no effect on our results.

f) The Evolutionary Tracks

i) Initial Models and the Zero-Age Main Sequence

The starting models for all evolutionary runs were "pre–main-sequence" uniform composition models, assumed to be in hydrostatic equilibrium with no gravitational energy generation. The initial ^3He abundance is very close to its *p-p* chain equilibrium abundance, but the CNO isotopes are far from their CNO cycle equilibrium abundances. In particular, ^{12}C is far above its equilibrium value relative to ^{14}N, and ^{13}C is far below its equilibrium value relative to ^{12}C. Thus the $^{12}C(p, \gamma)^{13}N(e^+\nu_e)^{13}C$ reaction contributes significantly to the energy generation at the star's center. There is a short (about 12 million year) and perhaps not very meaningful phase during which the star evolves slightly downwards and to the red in the H-R diagram, before reaching what may be considered the zero-age main sequence. Our models at this point had a small convective core ($\approx 0.036\ M_\odot$); inside this core, ^{13}C was in equilibrium relative to ^{12}C, but ^{12}C and ^{13}C were still far from equilibrium relative to ^{14}N.

The explanation for this pre–main-sequence behavior of our models is relatively straightforward. The $^{12}C(p, \gamma)^{13}N(e^+\nu_e)^{13}C$ reaction yields only 3.45 MeV, while the $^{13}C(p, \gamma)^{14}N$ reaction yields 7.55 MeV. Thus, initially, the growing ^{13}C abundance more than compensates for the declining ^{12}C abundance, and the total amount of energy generated by the sum of these two reactions grows. Since these reactions are *much* more temperature sensitive than the *p-p* chain, their energy generation is much more sharply peaked at the star's center. The increase in central energy generation causes the core to expand and cool slightly; this causes the *p-p* energy generation rate to decrease. Since most of the star's luminosity comes from the *p-p* chain, the star's luminosity decreases and the outer layers contract. When ^{13}C comes into equilibrium with ^{12}C (after about 12 million years) and both isotopes decline in concert, the central energy generation rate from their burning declines: the core thus contracts and heats, and the *p-p* chain burning rate increases, causing the total luminosity to increase and the outer layers of the star to expand. We consider this to be the zero-age main sequence point.

ii) Convergence to a Standard Sun

One of the objects of this paper was to obtain a value for the initial solar helium abundance Y. However, one must choose some specific composition values for any particular evolutionary sequence. For most of the comparison solar models, we chose to fix the metallicity Z and varied the initial helium abundance Y and the mixing length α until the model matched the observed solar luminosity $L_\odot$ and effective temperature T_e at the solar age $t_\odot$. To obtain a good standard Sun, we fixed the initial Z/X ratio at the Grevesse (1984) value of 0.02766, varying Y and Z in concert to maintain this ratio, and of course also varying α, until the model matched $L_\odot$ and T_e at the age $t_\odot$.

For all but one of our solar models we used the $L_\odot$ value given by Bahcall *et al.* (1982), namely $L_\odot \equiv (3.86 \pm 0.02) \times 10^{33}$ ergs s^{-1}; their determination included the results of the *Nimbus 7* satellite (Hickey *et al.* 1980) and the NASA *Solar Maximum Mission* Spacecraft (Willson *et al.* 1981), as well as two separate rocket flights (Willson, Duncan, and Geist 1980) and a weighted average of previous measurements (Willson and Hickey 1977). This resulted in $\log T_e = 3.7612$, as obtained from a blackbody with $L = L_\odot$ and $R = R_\odot \equiv (6.960 \pm 0.0007) \times 10^{10}$ cm (Allen 1963). We made certain that our models were within a tenth of a percent of these values at the solar age. For comparison purposes, we computed one solar model with the older Allen (1963) value for $L_\odot \equiv (3.90 \pm 0.04) \times 10^{33}$ ergs s^{-1}, which implies $\log T_e \equiv 3.7623$ (see § III).

For our Standard Sun case, we used a value of $t = 4.55 \times 10^9$ yr for the time from our initial model to our "present Sun"; this is the value obtained for the age of the meteorites (see, e.g., Wasserburg *et al.* 1977 and Wasserburg, Papanastassiou, and Lee 1980). Note that our initial models have a uniform chemical composition, and require about 12 million years of "pre-main-sequence" evolution to bring ^{13}C to equilibrium with ^{12}C in the core. (This would normally occur while the sun was contracting to its zero-age main sequence point.) Thus, counting from the zero-age main sequence, our models have ages of $t_\odot \approx (4.55\text{–}0.012)$ Gyr ≈ 4.54 Gyr. This is close to the age value of $t_\odot = (4.49 \pm 0.04)$ Gyr derived recently by Guenther (1989), who argued that the older meteorites must have formed during the pre-main-sequence stage while the Sun still had a dense accretion disk, so that the age of the sun must be *less* than the age of the oldest meteorites. The opposite has been commonly assumed, and ages of 4.6 Gyr (see, e.g., Bahcall and Ulrich 1988) or 4.7 Gyr (see, e.g., Bahcall *et al.* 1982) have been used. Fortunately, differences of this size in the solar age have very little effect on solar models. We used $t = 4.6$ Gyr (resulting in $t_\odot \approx 4.59$ Gyr) for four of our comparison solar runs and also tested the effect of varying the solar age by computing one solar model using $t = 4.7$ Gyr (resulting in $t_\odot \approx 4.69$ Gyr). We found that increasing the solar age by 0.1 Gyr had a negligible effect on the solar model (see § III).

iii) Space and Time Step Sizes in Our Models

The maximum difference that we allowed between adjacent layers of the model was 2% for temperature, radius, and luminosity, and 6% for density; the Henyey iterations were converged until changes in these quantities from one iteration to the next were less than 2×10^{-5} (or 6×10^{-5} for density), or to an accuracy of 10^{-4} in the equations of stellar structure, whichever came first (usually both were satisfied). The compositions X, Y, ^{12}C, and ^{16}O were allowed to change by 0.02, while ^{14}N, ^{13}C, ^{17}O, and ^{18}O were not allowed to change by more than 1% of Z. This resulted in 200–250 mass layers in the interior (i.e., $\log T \geq 6.3$, which comprises about 98% of the solar mass). The surrounding static envelope was integrated inwards numerically, starting at a density of $\log \rho = -12$, and using the same integration step size restrictions for temperature, radius, and density as in the interior; additionally, the step size in $(M - M_r)$ was restricted to 15%, the change in the number of free (ionized) electrons per nucleon was restricted to 0.02, and outside the photosphere the change in optical depth was restricted to 10%. This resulted in about 200 integration steps outside the photosphere, and about another 350 integration steps in the envelope.

The maximum allowed change in physical quantities and compositions for the same mass layer at successive time steps was the same as the maximum allowed difference between adjacent mass layers in the interior. There were some additional constraints on the size of the time step, but none of these had any effect on the time step except the constraint that the convective core should not change by more than 2% of its maximum extent (and this came into play only in the early main sequence, since the convective core disappeared at an age of about 60 million years). Due to these constraints on the time step size, about 130 time steps were needed to reach the solar age (the maximum time step size was about 125 million years, occurring just prior to the solar age: near the beginning of the evolution, time steps were considerably smaller).

III. RESULTS AND DISCUSSION

a) The Presolar Helium Abundance and Metallicity

We computed three self-consistent solar models with the Grevesse (1984) value of $Z/X = 0.02766$ and a solar age of $t_\odot = 4.54$ Gyr (first three rows of Table 2). For our *Standard Sun* (case 1) we obtain values for the presolar (initial) helium abundance and metallicity, and the convective mixing length to pressure scale height ratio, of

$$Y = 0.278\,, \quad Z = 0.0194\,, \quad \text{and } \alpha = 2.1\,. \qquad (4)$$

This is in excellent agreement with recent results of other authors: our Y value is close to the value of $Y = 0.281$ obtained by Guenther, Jaffe, and Demarque (1989) and the value of $Y = 0.276$ obtained by Turck-Chièze *et al.* (1988) (see Table 2). The value of Bahcall and Ulrich (1988) is somewhat lower, namely $Y = 0.271$. All these authors (like ourselves used the Grevesse (1984) Z/X ratio, and all used the LAOL opacities in the solar interior.

The earlier solar model of Bahcall *et al.* (1982) also obtained a somewhat low Y value, when they used the lower value of $Z/X = 0.0228$ (Ross and Aller 1976); even when they corrected Y to the value that *would* have been obtained using the Grevesse (1984) Z/X value, they still obtained a slightly low value, $Y = 0.267$ (see Bahcall and Ulrich 1988). This is a bit lower than their more recent value of $Y = 0.271$, perhaps due to the overcorrection of the Diesendorf (1970) reduction to the Thompson electron scattering used in their first paper. The reason why their Y values are consistently lower than those of other authors is not obvious. It is true that their outer boundary conditions are based on a grid of envelope calculations that use Vardya (1964) opacities, but we found that even very large differences in the atmospheric opacities have no effect on Y (see

TABLE 2

PRESOLAR COMPOSITION, CENTRAL CONDITIONS, AND PREDICTED ^{37}Cl NEUTRINO RATES

Model or Author	Age (Gyr)	$L_\odot$[a]	Y	Z	Z/X	T_c (10^6 K)	ρ_c (g cm^{-3})	X_c	$\nu(^{37}Cl)$ (SNU)
Present work:[b]									
1. Standard Sun	4.54	3.86	0.2783	0.01943	0.02766	15.43	146.6	0.3629	7.68
2. "dep. co."	4.54	3.86	0.2783	0.01943	0.02766	15.43	146.4	0.3634	7.66
3. High $L_\odot$	4.54	3.90	0.2793	0.01940	0.02766	15.48	147.8	0.3589	8.28
4. "fixed Z"	4.59	3.86	0.2803	0.02	0.02858	15.47	147.5	0.3573	7.97
5. "low κ"	4.59	3.86	0.2803	0.02	0.02858	15.48	147.5	0.3574	8.00
6. High age	4.69	3.86	0.2794	0.02	0.02855	15.50	149.0	0.3525	8.17
7. $\epsilon(^3He)_{nonequil}$	4.59	3.86	0.2816	0.02	0.02864	15.45	145.8	0.3580	7.81
8. Low (Z/X)	4.59	3.86	0.2619	0.016	0.02216	15.21	145.3	0.3819	5.92
Other authors:[c]									
1. Guenther 89	4.5	?	0.281	0.0194	0.0277	15.53[d]	145.7[d]	...	...
2. Bahcall 88	4.6	3.86	0.2706	0.01961	0.02763	15.6	148.	0.3411	7.9
3. Turck-Chièze 88	4.6	3.86	0.276	0.0197	0.0280	15.51	147.7	0.3550	5.8
4. Lattanzio 89	4.6	3.86	0.287	0.02	0.0289	15.62	145.7	0.3395	...
5. Cahen 86	4.57	3.86	0.285	0.02	0.02878	15.64	145.8	0.3474	7.4
6. Lebreton 86	4.6	3.86	0.282	0.02	0.02865	15.91	160.3	0.3353	13.3
7. Wambsganss 88	4.65	3.82	0.270	0.0189	0.02658	16.02	...	...	...
8. VandenBerg 83	4.7	3.90	0.27	0.0169?	0.0237?	...	...	...	8.3
9. Bahcall 82	4.7	3.86	0.252	0.0167	0.0228	15.50	156.3	0.3545	7.6

[a] Value used for the present solar luminosity, in units of 10^{33} ergs s^{-1}.

[b] See text for full description of these cases.

[c] Standard Sun reference model was chosen from among those given by each author. Full references: (1) Guenther, Jaffe, and Demarque 1989; (2) Bahcall and Ulrich 1988; (3) Turck-Chièze *et al.* 1988; (4) Lattanzio 1989; (5) Cahen, Doom, and Cassé 1986; (6) Lebreton and Maeder 1986; (7) Wambsganss 1988; (8) VandenBerg 1983; (9) Bahcall *et al.* 1982.

[d] The quoted values were given for a less accurate version of their standard model, with slightly different initial parameters.

§ IIIc below). Again, it is true that Bahcall and Ulrich (1988) used only seven time steps to reach the solar age; however, Guenther, Jaffe, and Demarque (1989) performed runs both with 10 and with 80 time steps and found very similar results for these two cases.

There are nonnegligible uncertainties in the solar age, luminosity, and composition, and different authors have used different values for these as shown (for recent papers) in Table 2. We investigated the effects of varying each of these in turn, as well as some effects having to do with the input physics of the solar model. Adding the effects of pressure ionization (case 2: "depression of the continuum") to the equation of state had *no effect* on the solar model, except that a slightly larger α was required (2.3 rather than 2.1). Increasing $L_\odot$ by 1% (case 3), which is twice the quoted uncertainty of Bahcall *et al.* (1982), led to only a small increase in Y (of 0.001).

To investigate the effects of the other uncertainties, we computed a number of solar models, changing one input at a time. For convenience, and to eliminate Z-interpolation in opacity tables, we arbitrarily chose to fix Z at a value of 0.02 (close to our solar value of 0.0194), rather than fixing Z/X; we also used a slightly different age (4.59 Gyr, which results from subtracting our pre–main-sequence time from an evolution time of 4.6 Gyr: see § II*f*[ii]). For these, our reference model is case 4 of Table 2. To test the effect of the large uncertainty in low temperature opacities (due to molecules), we artificially reduced the opacity at temperatures below 10^4 K by an amount $\Delta(\log \kappa) = (4 - \log T)/0.7$; this would amount to reduction in κ by a factor of 10 at $\log T = 3.3$ (the lowest temperature for which we had opacities), or slightly more than a factor of 2 at the solar photosphere. Surprisingly, in view of the large effects of interior opacities found by Guenther, Jaffe, and Demarque (1989), we found that even our extreme changes in the low-temperature opacities had absolutely *no effect* on the helium abundance Y and the interior quantities of our model, although they resulted in a considerable reduction in α (1.5 rather than 2.1). This is case 5 of Table 2. In contrast to us, Lebreton and Maeder (1986) *did* find a small effect when they replaced their molecular opacities (below 1 eV) with old opacities (without molecules): they stated that a reduction in Y of 0.003 was necessary to match $L_\odot$. However, they do not say whether they matched T_e in this model (by changing α). Changing α *does* have a small but not completely negligible effect on the luminosity, so that a model which matches only the solar luminosity but not the effective temperature will have a slightly incorrect value of Y. Note also that their changes in the low-temperature opacities were probably rather larger than ours, and also extended deeper into the star.

To check the effect of varying the solar age, we computed a solar model with the age increased by 0.1 Gyr (case 6 of Table 2). This resulted in a small decrease in Y of about 0.001.

We had always followed the nonequilibrium abundance of ^{3}He, but the *p-p* chain *energy generation rate* was always computed as if ^{3}He was at its equilibrium abundance. For one solar model, we investigated the effect of nonequilibrium ^{3}He energy generation (case 7 of Table 2). This again had only a small effect, causing an increase in Y of only about 0.001; however, we are not completely certain of the numerical stability of our present algorithm for including ^{3}He nonequilibrium energy generation; the true effect may be smaller.

We also computed a solar model with a lower Z value (of 0.016), which corresponds to a Z/X ratio of 0.0222, close to but slightly lower than the old Ross and Aller (1976) value of 0.0228 (case 8 of Table 2). This resulted in a *considerable* change in the solar Y value, reducing it by about 0.018. This change corresponds to

$$\frac{\partial Y}{\partial Z} = 4.6 \,, \quad \text{or} \; \frac{\partial Y}{\partial (Z/X)} = 2.8 \,, \quad \text{or} \; \frac{\partial \ln Y}{\partial \ln (Z/X)} = 0.28 \,. \quad (5)$$

This is in good agreement with the value of Bahcall and Ulrich

(1988): they give $\partial \ln Y/\partial \ln(Z/X) = 0.30$, obtained from Bahcall *et al.* (1982). We also agree well with Cahen (1986), who obtained $\partial Y/\partial Z = 4$. Guenther, Jaffe, and Demarque (1989) made changes in the abundances of the *individual* heavy elements, which resulted in a change in Z, but also in the *relative* abundances of the components of Z; they were the only authors up to now who computed the separate opacity contribution from each of the heavy elements. When they changed Ne (holding all other heavy elements fixed: see their Table 3), they found $\partial Y/\partial Z_{\mathrm{Ne}} \approx 4.1$, similar to the $\partial Y/\partial Z$ values of other authors. However, when they switched from $Z = 0.0169$ with the relative abundances of Ross and Aller (1976) to $Z = 0.0194$ with the relative abundances of Grevesse (1984) (using LAOL opacities in both cases), they obtained $\partial Y/\partial Z_{\mathrm{mix}} \approx 1.2$. This leads to the disturbing conclusion that the changes in the individual mixes cancelled most of the effect of changing Z as a whole. This is especially puzzling in that the largest difference in the makeup of Z was in Ne.

Three other recent papers used the same Z and same $L_\odot$ as our case 4, and almost the same age $t_\odot$ (see Table 2); they also used LAOL opacities. This allows another direct comparison of the resulting solar Y: we obtained $Y = 0.280$ for our case 4, while values of 0.287, 0.285, and 0.282 were obtained respectively by Lattanzio (1989), Cahen, Doom, and Cassé (1986), and Lebreton and Maeder (1986). Note that Cahen, Doom, and Cassé (1986) are the other three authors of Turck-Chièze *et al.* (1988), whose value of Y was slightly lower than ours.

Wambsganss (1988) and VandenBerg (1983) used different solar parameters from any of our cases (most importantly, different Z/X ratios: see Table 2). When we apply the shifts in Y (described above) caused by the different solar age, luminosity, and Z/X, we find that our model would have a Y value larger than that of Wambsganss (1988) by about 0.005, if we had matched his solar parameters; correspondingly, our Y value would be lower than that of VandenBerg (1983), by about the same amount. Note that Wambsganss (1988) investigated the effect of diffusion; he found that the presolar Y value was negligibly affected (being reduced by only 0.002), although diffusion further decreased the surface helium abundance by a non-negligible amount (about 0.014) over the solar age.

In conclusion, all recent papers (described in Table 2) point to a presolar helium content in the range $0.271 \leq Y \leq 0.285$ at the Grevesse (1984) value of Z/X, with our standard Sun having a value of $Y = 0.278$. Note that it mainly is one's choice of Z/X ratio that determines the value of Z: $Z = (1 - Y)(Z/X)[1 + (Z/X)]^{-1}$, where $(1 - Y) \sim 0.72$, so that $\Delta Z/Z \approx -\Delta Y/0.72$; thus variations in Y of order ± 0.01 change Z by only 1.4%. Thus all models using the Grevesse (1984) value of Z/X and LAOL opacities will result in similar values of Z, close to $Z \approx 0.0194$.

The presolar helium abundance should be larger than the primordial value. Boesgaard and Steigman (1985) give $Y_p = 0.239 \pm 0.015$, obtained from observations of Galactic and extragalactic H II regions. The inhomogeneous big bang computations of Malaney and Fowler (1988) give a similar value, namely $Y_p = 0.25 \pm 0.01$. Galactic chemical evolution will cause enhancement of both helium and metals. With our value of $Y = 0.278$ and $Z = 0.0194$ for the presolar nebula, we obtain $\Delta Y/\Delta Z = 2.0 \pm 0.8$ for the former value of Y_p, and $\Delta Y/\Delta Z = 1.5 \pm 0.5$ for the latter. These helium-to-metals enrichment ratios are in good agreement with galactic evolutionary models of Maeder (1984), who estimated $1 \lesssim \Delta Y/\Delta Z < 2.3$.

b) Central Conditions and the Neutrino Problem

Table 2 contains the central conditions for the standard solar models obtained in the present work as well as those of other authors. Most models find fairly similar central conditions. For our *Standard Sun* the predicted ^{37}Cl neutrino capture rate is 7.7 SNUs, consistent with the Bahcall and Ulrich (1988) value of 7.9 SNUs (note 1 SNU $\equiv 10^{-36}$ captures s^{-1} per target atom). Turck-Chièze *et al.* (1988) obtained a significantly lower value of 5.8 SNUs, partly due to their use of the Barker and Spear (1986) value for the $^7\mathrm{Be}(p, \gamma)$ cross section, which is 13% lower than the value we used (from Caughlan and Fowler 1988). Their earlier work (Cahen, Doom, and Cassé 1986), using the same cross section as we did, yielded a value of 7.4 SNUs, in fairly good agreement with our results and those of Bahcall and Ulrich (1988). Lebreton and Maeder (1986) obtained a high neutrino rate of 13.3 SNUs, presumably due to their unusually high central temperature.

From our different models, it is clear that uncertainties in the solar age and in molecular opacities have negligible effect on the neutrino rate (see Table 2), nor does inclusion of pressure ionization effects or nonequilibrium ^{3}He energy contributions have any significant effect. A fairly small increase of 0.6 SNUs resulted from a 1% increase in the value used for $L_\odot$. The largest effect was obtained from changing Z/X: using cases 4 and 8 of Table 2, one can calculate that reducing Z/X from the Grevesse (1984) value to the Ross and Aller (1976) value would result in a reduction in the ^{37}Cl neutrino capture rate of about 1.5 SNUs.

In all cases, ours and those of other authors, the theoretical models yield ^{37}Cl neutrino capture rates several times higer than the observed rate, which is 2.1 ± 0.3 SNU (Davis 1964, 1978; Rowley, Cleveland, and Davis 1985; Davis 1986; Davis *et al.* 1989). In other words, *the case of the missing solar neutrinos* (Fowler 1982) has not been solved by the standard solar models: one must invoke some "nonstandard" mechanism to reduce the predicted ^{37}Cl neutrino rate.

Bahcall and ulrich (1988) looked at some such "nonstandard" mechanisms. They considered the possibility of inhomogeneous solar composition, i.e., with $Y \sim 0.12$ and $Z \sim 0.0024$ throughout most of the interior; this model fixed the neutrino problem but was inconsistent with helioseismological data, let alone requiring a Y value a factor of 2 smaller than the big bang primordial value and a similarly unreasonable Z value. They also considered the possibility of additional energy transport in the solar interior by (hypothetical) weakly interacting massive particles (WIMPs) left over from the big bang: this also could fix the neutrino problem. There are other exotic possibilities, ranging from enhanced diffusion of elements (e.g., turbulent diffusion arising from differential rotation) to a postulated black hole at the Sun's center (see, e.g., Bahcall, Bahcall, and Ulrich 1969; Rood 1978; Schatzman and Maeder 1981; Schatzman 1985; Michaud 1985; Roxburgh 1985*a*, *b*; Cox, Kidman, and Newman 1985; Newman 1986; Lebreton 1986). Note that Cox, Kidman, and Newman (1985) and Lebreton (1986) both conclude that sufficient turbulent diffusion mixing in the core to solve the neutrino problem would lead to models inconsistent with solar oscillation data. Wambsganss (1988) showed that including pressure diffusion, temperature diffusion, and concentration diffusion of hydrogen and helium in a *non-rotating* solar model caused an increase in the central temperature, making the neutrino problem worse.